



LHC production of forward-center and forward-forward di-jets in the k_t -factorization and transverse dependent *unintegrated* parton distribution frameworks

M. Modarres^{a,*}, M.R. Masouminia^{a,1}, R. Aminzadeh Nik^a,
H. Hosseinkhani^b, N. Olanj^c

^a Department of Physics, University of Tehran, 1439955961, Tehran, Iran

^b Plasma and Fusion Research School, Nuclear Science and Technology Research Institute, 14395-836 Tehran, Iran

^c Physics Department, Faculty of Science, Bu-Ali Sina University, 65178, Hamedan, Iran

Received 18 February 2017; received in revised form 18 June 2017; accepted 25 June 2017

Available online 29 June 2017

Editor: Hong-Jian He

Abstract

The present work is devoted to study the high-energy *QCD* events, such as the di-jet productions from proton–proton inelastic collisions at the *LHC* in the forward-center and the forward-forward configurations. This provides us with much valuable case study, since such phenomena can provide a direct glimpse into the partonic behavior of a hadron in a dominant gluonic region. We use the *unintegrated* parton distribution functions (*UPDF*) in the k_t -factorization framework. The *UPDF* of Kimber et al. (*KMR*) and Martin et al. (*MRW*) are generated in the leading order (*LO*) and next-to-leading order (*NLO*), using the Harland-Lang et al. (*MMHT2014*) *PDF* libraries. While working in the forward-center and the forward-forward rapidity sectors, one can probe the parton densities at very low longitudinal momentum fractions (x). Such a model computation can provide simpler analytic description of data with respect to existing formalisms such as perturbative *QCD*. The differential cross-section calculations are performed at the center of mass energy of 7 TeV corresponding to *CMS* collaboration measurement. It is shown that the gluonic jet productions are dominant and a good description of data as well as other theoretical attempts (i.e. *KS*-linear, *KS*-nonlinear and *rcBK*) is obtained. The uncertainty of the calculations is derived by manipulating the hard scale of the processes by a factor of two. This conclusion is achieved, due to the particular visualization of the angular ordering constraint (*AOC*), that is incorporated in the definition of these *UPDF*.

* Corresponding author. Fax: +98 21 88004781.

E-mail address: mmodares@ut.ac.ir (M. Modarres).

¹ Visiting the Institute of Nuclear Physics, Polish Academy of Science, Krakow, Poland.

© 2017 The Authors. Published by Elsevier B.V. This is an open access article under the CC BY license (<http://creativecommons.org/licenses/by/4.0/>). Funded by SCOAP³.

1. Introduction

Analyzing the raw data, which comes pouring out of the *LHC*, presents a challenge of considerable proportions, given that the dynamics of the true players in the hadronic inelastic collisions, i.e. partons, are shadowed by the laws of strong interactions. However, to understand the nature of our universe, it is paramount to enlighten the behavior of these fundamental substances. Gluonic saturation in hadron evolution is the subject of on-going investigations in the study of the *QCD*. This phenomenon which is a consequence of perturbative unitarity of the hadronic evolution equations, is related to the rate of growth of the cross section with respect to the energy of the collision.

Amazingly, an answer came a few decades ago, in the form of the *Dokshitzer–Gribov–Lipatov–Altarelli–Parisi (DGLAP)* evolution equations, [1–4],

$$\begin{aligned} \frac{d}{d\log(\mu^2)} g(x, \mu^2) &= \frac{\alpha_s(Q^2)}{2\pi} \int_x^1 \frac{dz}{z} \left[P_{gg}^{(LO)}\left(\frac{x}{z}\right) g(z, \mu^2) + P_{qg}^{(LO)}\left(\frac{x}{z}\right) \sum_q q(z, \mu^2) \right], \\ \frac{d}{d\log(\mu^2)} q(x, \mu^2) &= \frac{\alpha_s(\mu^2)}{2\pi} \int_x^1 \frac{dz}{z} \left[P_{qq}^{(LO)}\left(\frac{x}{z}\right) q(z, \mu^2) + P_{qg}^{(LO)}\left(\frac{x}{z}\right) g(z, \mu^2) \right]. \end{aligned} \quad (1)$$

$g(x, \mu^2)$ and $q(x, \mu^2)$ as the solutions of the *DGLAP* evolution equations, are single-scale parton density functions (*PDF*), corresponding to gluons and quarks, respectively (they are presented by $a(x, \mu^2)$ in this work). These solutions depend on the fraction of the longitudinal momentum of parent hadron (x) and an ultra-violet cutoff (μ^2), which denotes the virtuality of the particle that is being exchanged throughout the inelastic scattering (*IS*). $P_{ab}^{(LO)}$ are the LO splitting functions (see the [Appendix A](#)). α_s represents the *LO* running coupling constant of the strong interaction which depends on, μ^2 , the number of involving flavors, n_f , and the *QCD* fundamental low energy scale, Λ_{QCD} [5]. The value of the Λ_{QCD} , usually around 300 MeV, can be effectively extracted from experiment. The terms on the right-hand side of the equation (1), correspond to the real emission and the virtual contributions, respectively.

The main postulation in the *DGLAP* evolution equation, i.e. the strong ordering hypothesis, is to neglect the transverse momenta of the partons along the evolution ladder, and to sum over the $\alpha_s \ln(\mu^2)$ contributions. One finds out that neglecting the contributions that come from this transverse dependency may harm the precision of the calculations, particularly in the high-energy processes and in the small- x region [6–16]. Hence, the need for introducing some transverse momentum dependent (*TMD*) evolution equation becomes apparent. This gave rise to the *Ciafaloni–Catani–Fiorani–Marchesini (CCFM)* and the *Balitski–Fadin–Kuraev–Lipatov (BFKL)* evolution equations [17–26].

One of the main features of the *CCFM* evolution equation is that it employs a physical constraint, to ensure that the gluons emissions are accompanied by a constant increase in the angle of the emission. This feature which is known as the angular ordering constraint (*AOC*), is related to the color coherent radiations of the gluons. The solutions of the *CCFM* equation, $f(x, k_t^2, \mu^2)$

is a double-scaled *TMD PDF*, which in addition to the x and Q , depends on the transverse momentum of the incoming partons, k_T . The idea behind the *CCFM* evolution equation (to make the use of the *AOC* in the evolution ladder) is valid only in the case of gluon-dominant processes, i.e. in the small- x sector. If the proper physical boundaries are inserted, the *CCFM* equation will reduce to the conventional *DGLAP* and *BFKL* evolutions [27].

Mathematically speaking, solving the *CCFM* equation is rather difficult, usually possible with the help of Monte Carlo event generators [28,29]. On the other hand, the main feature of the *CCFM* equation, i.e. the *AOC*, can be used only for the gluon evolution and therefore, producing convincing quark contributions in this framework is only a recent development, see the references [30–32]. Given these complexities, Martin et al., employed the idea of *last-step* evolution along the k_T -factorization framework, [6–11], and developed the *Kimber–Martin–Ryskin (KMR)* and the *Martin–Ryskin–Watt (MRW)* approaches [12,13]. Both of these formalisms are constructed around the solutions of the *LO DGLAP* evolution equations and modified with different visualizations of the angular ordering constraint. These *UPDF* have been widely used to describe different *QCD* related high-energy events, e.g. [33–41]. On the other hand, such a model computation can provide a simpler analytic description of data with respect to other complicated existing formalisms such as perturbative *QCD* etc.

One extraordinary test-ground for the *UPDF* of the k_T -factorization is the probe of the forward-center and forward-forward rapidity sectors in the hadronic collisions, given that it involves the dynamics of the small- x region, e.g. $x \sim 10^{-4}$ – 10^{-5} , where the gluon density dominates. Since the decisive difference between the *UPDF* of *KMR* and *MRW* is in the different manifestations of the *AOC*, one could argue that working in such phenomenological setups could potentially exploit this diversity and unveil the true capacities of the presumed frameworks. For this propose, we have calculated the process of production of di-jets in the inelastic proton–proton collisions from the forward-center and the forward-forward rapidity regions, utilizing the *UPDF* of *KMR* and *MRW* in the *LO* and the *NLO*. Comparing these results with each other, and the results of the similar calculations in other frameworks, namely the linear and non-linear *KS* formalisms, [42–47], and with the experimental data from the *CMS* collaboration [48,49], would provide an excellent opportunity to study the strength and the weaknesses of the *UPDF* in the k_T -factorization framework.

The outlook of this paper is as follows: In the [Appendix A](#), we present a brief introduction to the framework of k_T -factorization and develop the required prescriptions for the *KMR* and the *MRW UPDF*, stressing their key differences regarding the involvement of the *AOC* in their definitions. The *UPDF* will be prepared in their proper k_T -factorization schemes using the *PDF* of *Harland-Lang et al. (MMHT2014)* in the *LO* and the *NLO*, [50]. The section 2 contains a comprehensive description over the utilities and the means for the calculation of the k_T -dependent cross-section of the di-jets production in the p – p *IS* processes. The necessary numerical analysis will be presented in the section 3, after which a thorough conclusion will follow in the section 4.

2. The di-jet production in the p – p collisions at the *LHC*

Generally speaking, the main contributions into the hadronic cross-section of the di-jet productions at the *LHC*, i.e.,

$$P_1 + P_2 \rightarrow J_1 + J_2 + X,$$

are the *LO* partonic sub-processes:

$$\begin{aligned}
 g(\mathbf{k}_1) + g^*(\mathbf{k}_2) &\rightarrow g(\mathbf{p}_1) + g(\mathbf{p}_2), \\
 g(\mathbf{k}_1) + g^*(\mathbf{k}_2) &\rightarrow q(\mathbf{p}_1) + \bar{q}(\mathbf{p}_2), \\
 q(\mathbf{k}_1) + g^*(\mathbf{k}_2) &\rightarrow q(\mathbf{p}_1) + g(\mathbf{p}_2).
 \end{aligned}
 \tag{2}$$

Since we are considering the forward sector for the partons that are produced in the k_t -factorization, the stated partons in the equation (2), one can safely neglect the qq and $q\bar{q}$ sub-processes.

To derive the master equation for the total cross-section of the production of di-jets in the framework of k_t -factorization, we can write,

$$\begin{aligned}
 &\sigma_{p-p}(P_1 + P_2 \rightarrow J_1 + J_2) \\
 &= \sum_{a,c,d=q,g} \frac{1}{1 + \delta_{cd}} \int \frac{p_{1,t} p_{2,t}}{8\pi^2(x_1 x_2 s)^2} dy_1 dy_2 \frac{dp_{1,t} dp_{2,t}}{k_t^2} d\Delta\varphi a(x_1, \mu^2) \\
 &\quad \times f_g(x_2, k_t^2, \mu^2) |\mathcal{M}_{a+g \rightarrow c+d}(x_1, \mu^2; x_2, k_t^2)|^2
 \end{aligned}
 \tag{3}$$

in which $p_{i,t}$ and y_i are the transverse momenta and the rapidities of the product particles and x_i are given as follows:

$$\begin{aligned}
 x_1 &= \frac{1}{\sqrt{s}} (p_{1,t} e^{+y_1} + p_{2,t} e^{+y_2}), \\
 x_2 &= \frac{1}{\sqrt{s}} (p_{1,t} e^{-y_1} + p_{2,t} e^{-y_2}).
 \end{aligned}
 \tag{4}$$

Additionally, the transverse momentum of the hybrid framework, k_t , is,

$$k_t = \left[p_{1,t}^2 + p_{2,t}^2 + 2p_{1,t} p_{2,t} \cos(\Delta\varphi) \right]^{1/2},
 \tag{5}$$

where $\Delta\varphi = \varphi_1 - \varphi_2$. $\mathcal{M}_{a+g \rightarrow c+d}$ are the matrix elements of the partonic sub-processes (see the references [44,46,47] to find analytic definitions of these quantities).

The term $1/(1 + \delta_{cd})$ restrains the over-counting indices. Note that, the existence of the term k_t^{-2} in the equation (3) is the remnant of the re-summation factor, dk_t^2/k_t^2 and since we are interested to look for the transverse momentum dependent jets with $p_{i,t} > 20$ GeV, the presence of such denominator would not cause any complication in the master equation. Additionally, we have to decide how to validate our *UPDF* in the non-perturbative region, i.e. where $k_t < \mu_0$ with $\mu_0 = 1$ GeV. A natural option would be to fulfill the requirement that:

$$\lim_{k_t^2 \rightarrow 0} f_g(x, k_t^2, \mu^2) \sim k_t^2,$$

and therefore, one can safely choose the following approximation for the non-perturbative region:

$$f_g(x, k_t^2 < \mu_0^2, \mu^2) = \frac{k_t^2}{\mu_0^2} x g(x, \mu_0^2) T_g(\mu_0^2, \mu^2).
 \tag{6}$$

In the next section, we will introduce some of the numerical methods that have been used for the calculation of the cross-section of the production of di-jets, using the *UPDF* of *KMR* and *MRW*.

3. The numerical analysis

We perform the 5-fold integration of the master equation (3), using the VEGAS algorithm in Monte-Carlo integration. To do this, we have selected the hard-scale of the *UPDF* as the share of each of the parent hadrons from the total energy of the center-of-mass frame:

$$\mu = \frac{1}{2} E_{CM}. \quad (7)$$

Varying this normalization value around a factor of 2, will provide each framework with a decent uncertainty bound. One would also set the upper boundaries on the transverse momentum integrations to $p_{i,max} = 4\mu$, noting that increasing this upper value does not have any effect on the outcome.

The forward rapidity sectors is conventionally defined as,

$$3.2 < |\eta_f| < 4.8, \quad (8)$$

where η denotes the pseudorapidity of a produced particle. Alternatively, to work in the central rapidity sector, one have to choose,

$$|\eta_c| < 2.8. \quad (9)$$

Moreover, as a consequence of employing the inclusive scenario (i.e. $p_{i,t} > 35$ GeV and limiting the rapidity integrations to the forward or central regions), one must assure that the produced jets must lie within this specific region. Thus, in order to cut-off the collinear and the soft singularities, it is conventional to use the anti- k_t algorithm [51], with radius $R = 1/2$, bounding the jets to this particular initial setup, through inserting a constraint on the y - ϕ plane:

$$R > \left[(\Delta\phi)^2 + (y_2 - y_1)^2 \right]^{1/2}. \quad (10)$$

Introducing the anti- k_t jet constraint ensures the production of 2 separated jets and rejects any single-jet scenarios.

4. Results, discussions and conclusions

Having in mind the theory and the notions of the previous sections and appendices A and B, we are able to calculate the production rates belonging to the di-jets in the forward-center and the forward-forward rapidity sectors, from the perspective of the k_t -factorization framework, utilizing the *UPDF* of *KMR* and *MRW*. The *PDF* of *Harland-Lang et al. [50]*, *MMHT2014*, in the *LO* and *NLO* levels, are used as the input functions for the unintegrated gluon densities, i.e., the equations (A.2), (A.4) and (A.9). Additionally, they are fit to be used as the solutions of the *DGLAP*, the *PDF* of the collinear factorization, directly in the master equation (3). We tend to perform the above calculations in any of our presumed frameworks, the *KMR*, the *LO MRW* and the *NLO MRW* (see the Fig. 1 for their gluonic *UPDF* and Appendix A for their definitions), then compare the results to each other, to the similar calculations in other frameworks and to the existing experimental data, in the case of the forward-center. See also Fig. 2.

So, the Figs. 3, 4 and 5 present the reader with the differential cross-section for the production of well-separated forward-central di-jets ($d^2\sigma/dp_t d\eta$), plotted against the transverse momentum of the corresponding jets (p_t) in the *KMR*, the *LO MRW* and the *NLO MRW* schemes respectively. The uncertainty bounds are calculated, varying the hard scale of the *UPDF* with a factor of 2, since this is the only arbitrary physical parameter in the framework of k_t -factorization. The

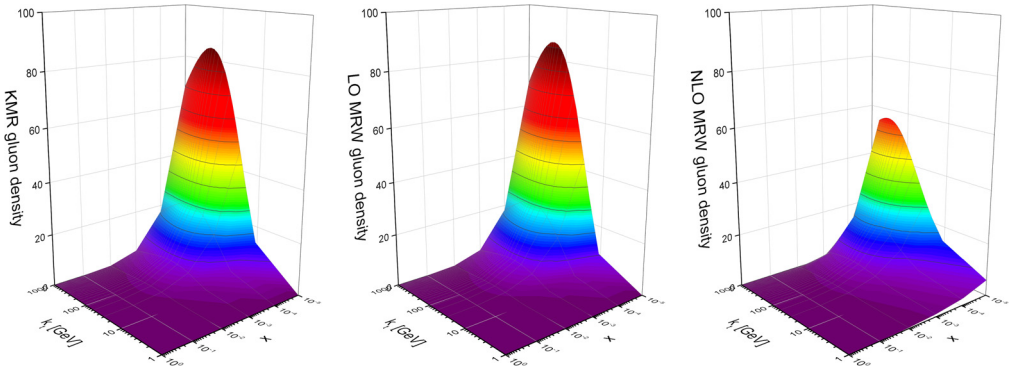


Fig. 1. The gluonic *UPDF* of the k_t -factorization versus the fractional longitudinal momentum of the parent hadron (x) and the transverse momentum of the parton, appearing on the top of the evolution ladder (k_t) at $\mu = 100$ GeV. The difference in the behavior of the *UPDF* in different frameworks is a direct consequence of employing different manifestations of the *AOC* in their respective definitions. To plot these diagrams we have used the *PDF* libraries of *MMHT2014* in the *LO* and the *NLO* as the input for the equations (A.2), (A.4) and (A.9).

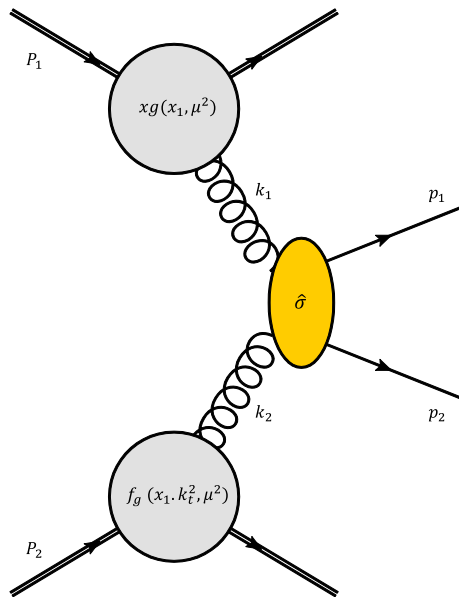


Fig. 2. The deep inelastic scattering of two protons in the forward-center configuration. The diagram shows the $g^* + g \rightarrow q + \bar{q}$ sub-process, assuming that one of the quarks is being produced in the forward sector (bounded by $3.2 < |\eta_f| < 4.7$) and the other in the center sector (bounded by $|\eta_c| < 2.8$). The parton density related to the first proton is being described with the *integrated PDF* while the second parton is prepared using the *UPDF* in one of our presumed frameworks.

blue-hatched pattern, the green-checked and the red-vertically striped patterns illustrate the individual contributions of the partonic sub-processes from the equation (2), corresponding to the $g^* + g \rightarrow g + g$, $g^* + g \rightarrow q + \bar{q}$ and $g^* + q \rightarrow g + q$ processes respectively. The black-horizontally striped pattern represents the sum of the sub-contributions. The calculations have been compared against the experimental data of the *CMS* collaboration, the reference [48]. One

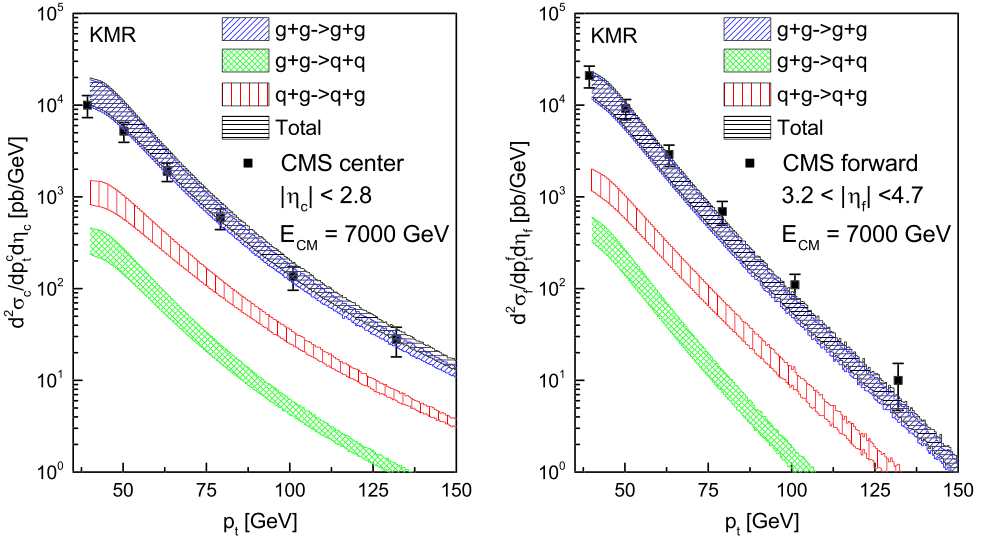


Fig. 3. The differential cross-section for the production of di-jets in the forward-center rapidity sector, calculated in the *KMR* framework for $E_{CM} = 7$ TeV. The contributions from each of the involving sub-processes from the equation (2) have been plotted separately. The black-oblique patterned histograms illustrate the sum of the partonic contributions. To determine the uncertainty of the calculations, we have manipulated the hard scale of the *UPDF*, $\mu = E_{CM}/2$, by a factor of 2. The data point are from the measurements of the *CMS* collaboration, the reference [48]. (For interpretation of the colors in this figure, the reader is referred to the web version of this article.)

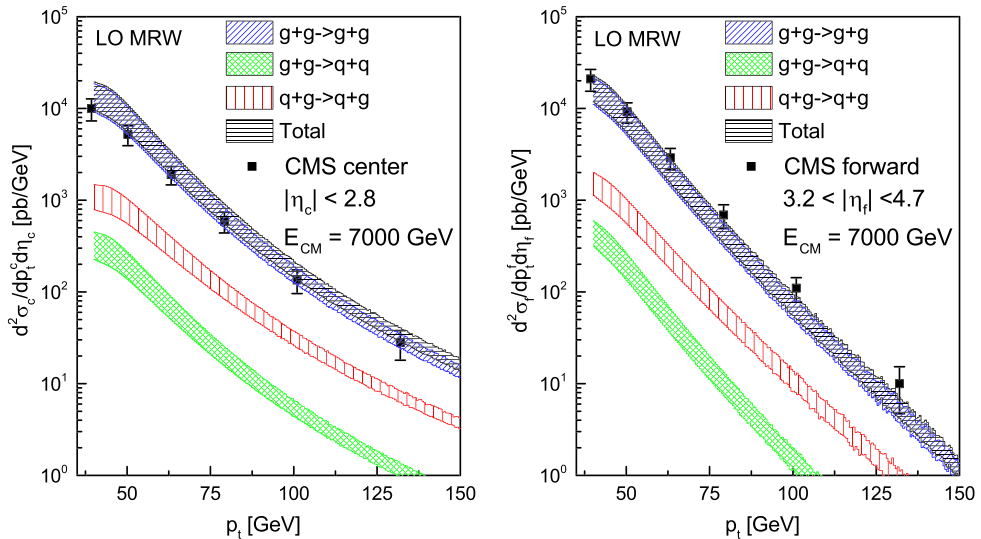


Fig. 4. The differential cross-section for the production of di-jets in the forward-center rapidity sector, calculated in the *LO MRW* framework. The notion of the diagrams are as in the Fig. 3. (For interpretation of the colors in this figure, the reader is referred to the web version of this article.)

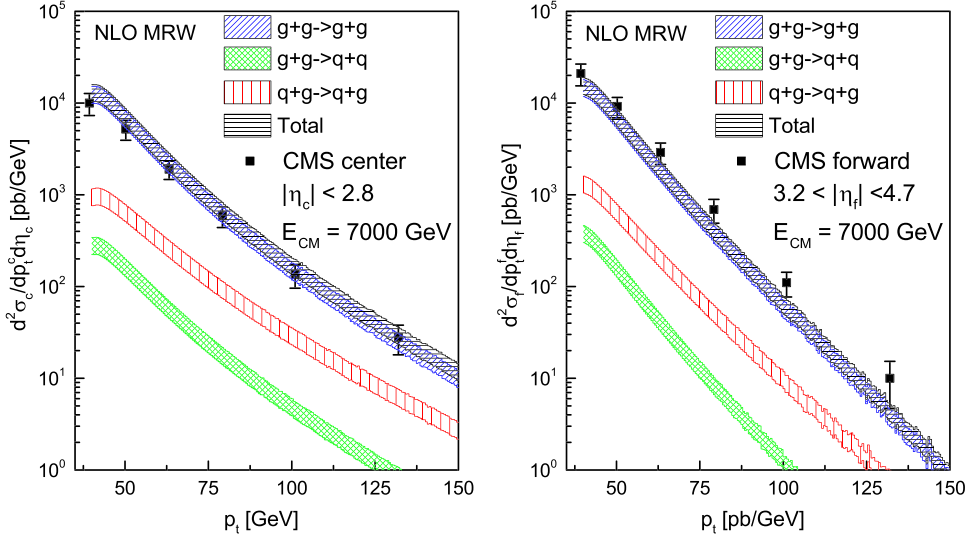


Fig. 5. The differential cross-section for the production of di-jets in the forward-center rapidity sector, calculated in the *NLO MRW* framework. The notion of the diagrams are as in the Fig. 3. (For interpretation of the colors in this figure, the reader is referred to the web version of this article.)

immediately notices that the share of the $g^* + g \rightarrow g + g$ sub-process dominates, relative to the negligible shares of the remaining two sub-processes. Although all of these frameworks are relatively successful in describing the experimental data, see the Fig. 6, it is interesting to find that the *UPDF* of *KMR* do as well as (if not better than) the *UPDF* of *MRW* in predicting the experimental results. The closeness of the behavior of different frameworks is a consequence of our choice for the hard scale of the *UPDF*, the equation (7). In order to enlighten this point, the Fig. 7 illustrates the result of making different choices in such calculations, using the *UPDF* of the *KMR*. To demonstrate the effect of changing the hard scale of the *UPDF* in the outcome, the histograms are calculated utilizing the following hard scale prescriptions

$$\begin{aligned}
 a) \quad & \mu = \frac{1}{2} (p_{1,t} + p_{2,t}), \\
 b) \quad & \mu = \frac{1}{2} (p_{1,t}^2 + p_{2,t}^2)^{1/2}, \\
 c) \quad & \mu = \text{Max}(p_{1,t}, p_{2,t}), \\
 d) \quad & \mu = \frac{1}{4} E_{CM}, \\
 e) \quad & \mu = \frac{1}{2} E_{CM}, \\
 f) \quad & \mu = E_{CM},
 \end{aligned} \tag{11}$$

where $\text{Max}(p_{1,t}, p_{2,t})$ returns the higher value between the transverse momenta of the produced jets. To save computation time, we only considered the contributions coming from the dominant $g^* + g \rightarrow g + g$ sub-processes. The choice *a*, which have been used in the similar calculations (e.g., the references [42–46] in the high energy factorization, from the point of view of the *UPDF* of the color glass condensation, (*CGC*)) proves to be in contrast with the particular manifestation

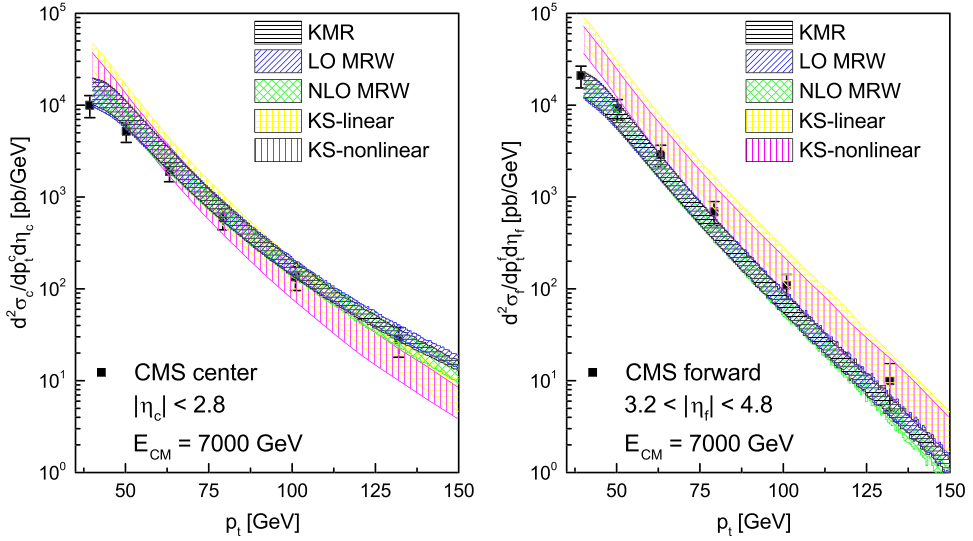


Fig. 6. The comparison between the differential cross-sections of the production of di-jets from the forward-center rapidity sector, in the different frameworks of the k_T -factorization. The results have been prepared as the numerical solutions the equation (3), using the *UPDF* of *KMR* and *MRW* in the *LO* and *NLO* with $E_{CM} = 7$ TeV. The data points are from the *CMS* report [48]. The yellow-checked and the purple-vertically striped patterns represent the calculations in the linear and non-linear *KS* frameworks, respectively, see the reference [42]. (For interpretation of the colors in this figure, the reader is referred to the web version of this article.)

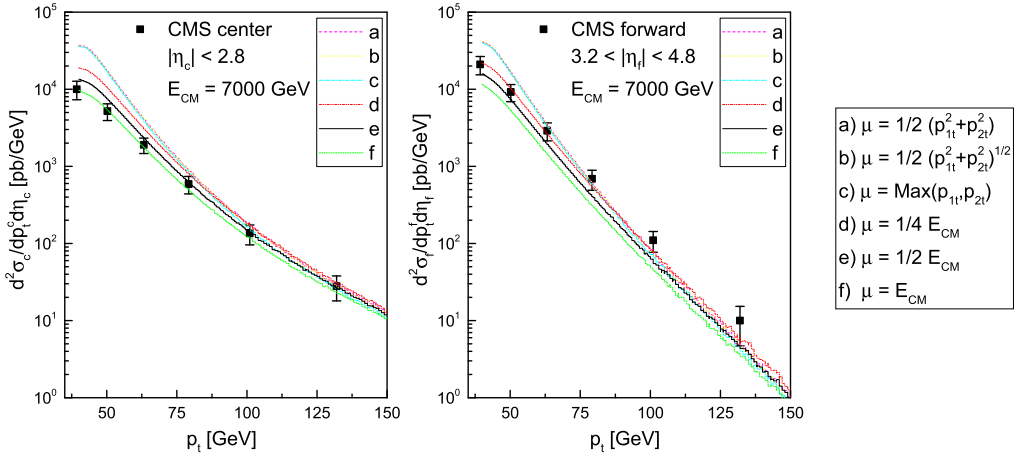


Fig. 7. The differential cross-section for the production of di-jets in the forward-center rapidity sector, for different choices of the hard scale and from the dominant $g^* + g \rightarrow g + g$ sub-process. The calculations have been carried on in the *KMR* framework for $E_{CM} = 7$ TeV. The histograms *a* through *f* have been calculated using the conditions from the equation (11). We have chosen the condition *e* (the black-continues histograms), i.e. the equation (7), as the primary prescription throughout this work.

of the *AOC*, specially in the case of *NLO MRW UPDF*. This is in addition to the considerable off-shoot of the results in the smaller values of the transverse momenta belonging to the produced jets. In the Fig. 6, the yellow-checked and the purple-vertically striped patterns represent the

calculations in the linear and the non-linear *KS* frameworks, respectively. The above separation between the predictions of the *KS* framework and the experimental data is apparent. To avoid such complications, we have chosen the condition e , in the equation (11), as the primary prescription for the hard scale of our *UPDF* throughout this work, see the section 3.

Having a closer look into the Fig. 6, one notices that such off-shooting results also appear in our settings for the production of di-jets. This is perhaps because of the over-simplified dynamics that have been used to derive these measurements. An increase in the precision may be realized via including higher order diagrams and introducing the final state parton showers in this frameworks [52]. Beside this point, note that our results show an acceptable agreement with the experimental data of the *CMS* collaboration, reference [48]. Another interesting observation is that in the large k_t , where the higher order corrections become important, the calculations in the *KMR* approach start to separate from the *LO MRW* and behave similar to the *NLO MRW*. The reason is that the inclusion of the *non-diagonal* splitting functions into the domain of the *AOC* introduces some corrections from the *NLO* region (in the form of $\ln(1/x)$ re-summations) into the *KMR* formalism.

A recent report from the *CMS* collaboration, the reference [49], concerns the angular distribution of the produced jets in the forward-center rapidity sector from a deep inelastic event at the *LHC*. Making use of this new information, we have calculated the differential cross-section of the forward-central di-jet production ($d\sigma/d\Delta\varphi$), plotted in the Fig. 8 against the angular difference of the produced partons (or equivalently the angular difference of the produced jets, $\Delta\varphi$). The panels (a), (b) and (c) in this figure illustrate the details of the calculations in each framework, consisting of the individual contributions of the sub-processes and the corresponding uncertainty bounds. The panel (d) presents the reader with the comparison of the total amounts in the presumed formalisms to each other and to the data from the reference [49]. Again, the results in the *KMR* approach seems to be equally good (or better than) those from the *MRW* in the *LO* or the *NLO*.

After proving the success of our formalism in describing the experimental data for the production of di-jets in the forward-center rapidity region, we can move forward with the prediction of a similar event, in the forward-forward sector, i.e. by choosing the rapidity of the produced jets (y_1 and y_2) to be both in the boundaries that where specified within the equation (8). Therefore, in the Fig. 9 the reader is presented with our predictions regarding the dependency of the differential cross-section of the forward-forward di-jet production ($d\sigma_f/dp_t^f$) to the transverse momenta of the produced jets (p_t), in the framework of k_t -factorization. The panels (a), (b) and (c) of the figure illustrate these predictions in the *KMR*, the *LO MRW* and the *NLO MRW* formalisms, respectively. The contributions of the individual partonic sub-processes are included. These contributions have the same general behavior as in the forward-central case, in spite of the fact that the measured contribution for the $g^* + g \rightarrow g + g$ and the $g^* + q \rightarrow g + q$ sub-processes are closer, compared to their counterparts from the forward-center region,

$$\begin{aligned} \hat{\sigma}_{F-C}(g^* + g \rightarrow g + g) &\gg \hat{\sigma}_{F-C}(g^* + q \rightarrow g + q) \gg \hat{\sigma}_{F-C}(g^* + g \rightarrow q + \bar{q}), \\ \hat{\sigma}_{F-F}(g^* + g \rightarrow g + g) &\gtrsim \hat{\sigma}_{F-F}(g^* + q \rightarrow g + q) \gg \hat{\sigma}_{F-F}(g^* + g \rightarrow q + \bar{q}). \end{aligned} \quad (12)$$

In addition, one can clearly perceive the effect of the $\Theta(1 - z - (k_t^2/\mu^2))$ constraint in the *NLO MRW* results, causing a steep descend in the corresponding histograms, in contrast with the behaviors of the results of the *KMR* and the *LO MRW* formalisms. Again, the similarity of the predictions of the *KMR* and the *LO MRW* schemes are a consequence of our choice of the hard scale, μ . Such similarity was also observed else where, e.g. the references [39–41], specially in the smaller x domains.

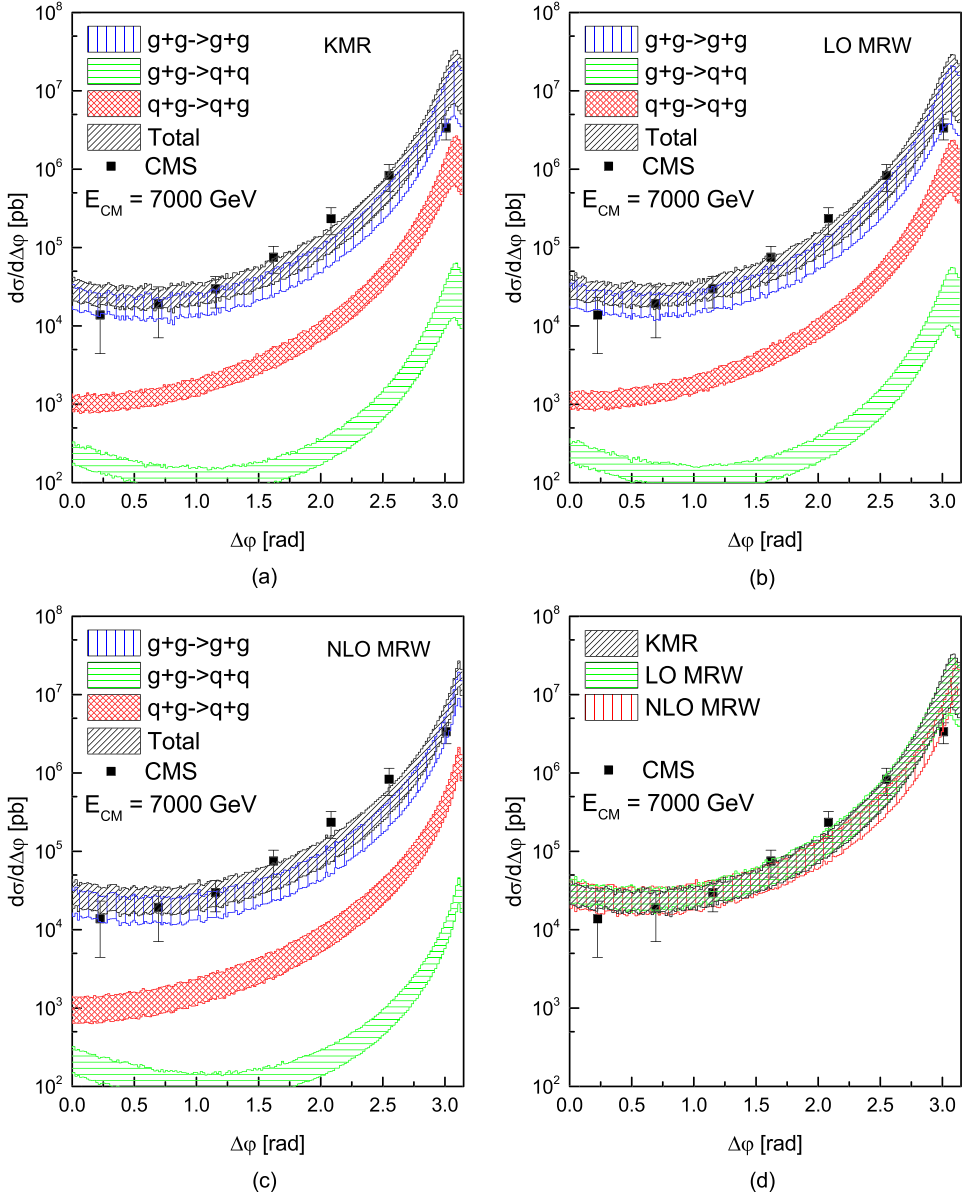


Fig. 8. The differential cross-section for the production of di-jets versus the angle of the out-coming jets, $\Delta\phi$. The calculations are in the forward-center rapidity sector for $E_{CM} = 7$ TeV. The panels (a), (b) and (c) illustrate the calculations, utilizing the *UPDF* of *KMR*, *LO MRW* and *NLO MRW*, respectively. The contributions from each of the involving sub-processes are shown separately. The panel (d) presents the comparison of these measurements against each other as well as the experimental data of the *CMS* collaboration, the reference [49]. The uncertainty of the calculations are provided through manipulating the hard scale of the *UPDF* by a factor of 2.

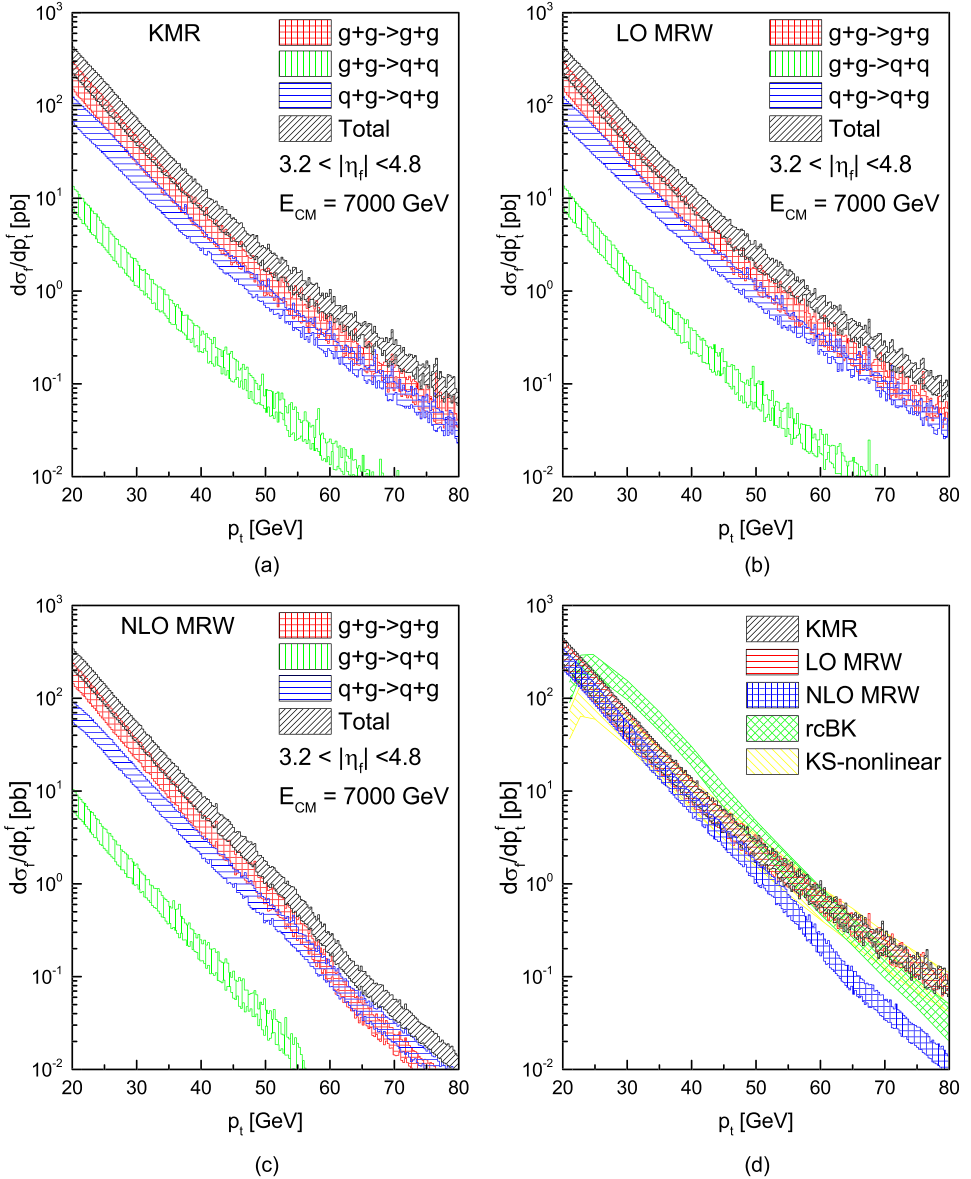


Fig. 9. The calculated predictions for the production of forward-forward di-jets in the framework of k_T -factorization with the central-mass energy of 7 TeV. The differential cross-section for the production of di-jets are plotted against the transverse momenta of the produced jets, in the *KMR*, *LO MRW* and *NLO MRW* schemes (i.e. the panels (a), (b) and (c), respectively), demonstrating the contributions of the individual sub-processes. The uncertainty bound is determined by manipulating the hard scale of the *UPDF*, $\mu = E_{CM}/2$, by a factor of 2. The panel (d) represents a comparison between the results of the k_T -factorization with the results from other frameworks, namely the Balitsky–Kovchegov *TMD PDF* convoluted with running coupling corrections (*rcBK*, see the references [53,54]) and the Kutak–Sapeta *TMD PDF* (*KS-nonlinear*, reference [46]).

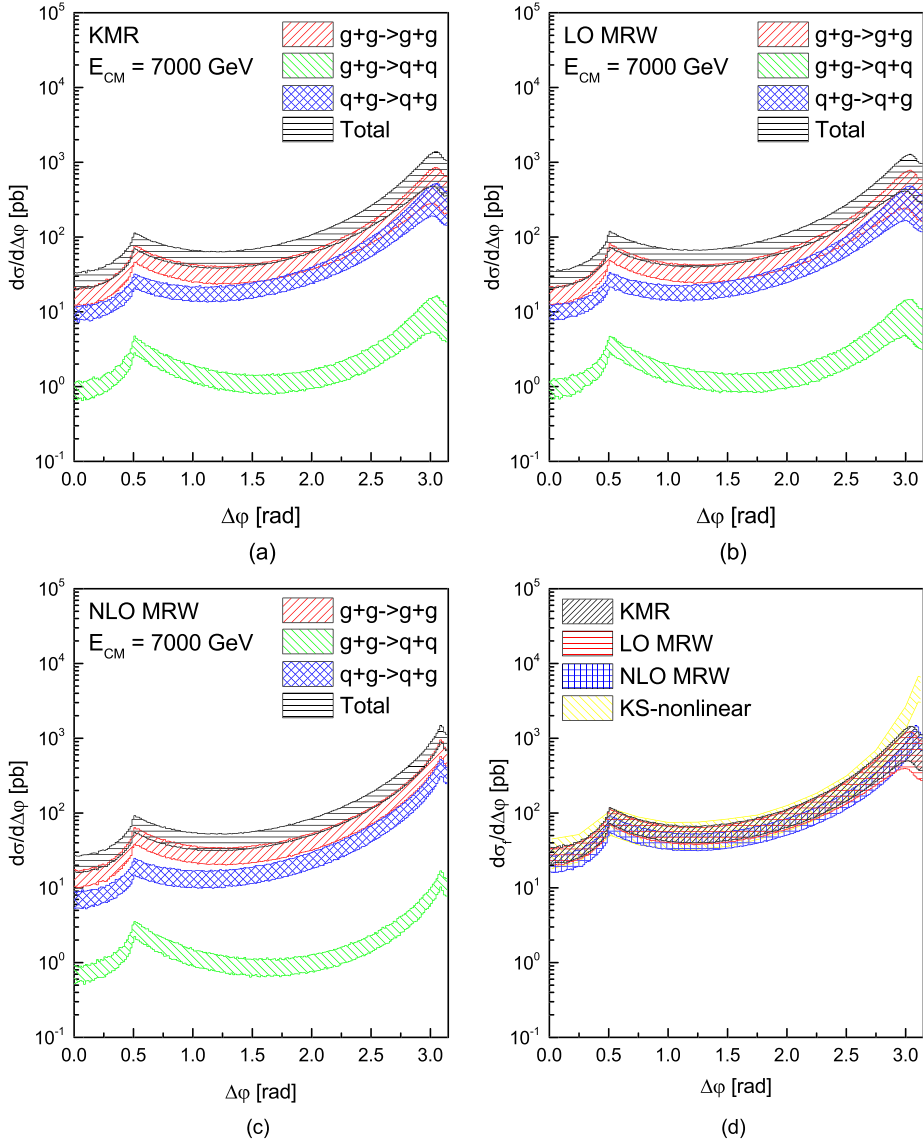


Fig. 10. The calculated predictions regarding the dependency of the differential cross-section for the production of forward-forward di-jets to $\Delta\phi$ using the $UPDF$ of k_T -factorization for $E_{CM} = 7$ TeV. The notion on the diagrams are as in the Fig. 9. In the panel (d), we have compared our results with the predictions made using the nonlinear KS TMD PDF from the reference [46].

The panel (d) of the Fig. 9 represents a comparison between the results of the k_T -factorization with the results from other frameworks, namely the *Balitsky–Kovchegov* TMD PDF convoluted with the running coupling corrections ($rcBK$, see the references [53,54]) and the *Kutak–Sapeta* TMD PDF (KS), the reference [44]. Both of these frameworks are specially designed to describe the behavior of the small- x region, incorporating the non-linear evolution of the *unintegrated* parton densities with the KS framework and the high energy factorization (HEF) formalism, in

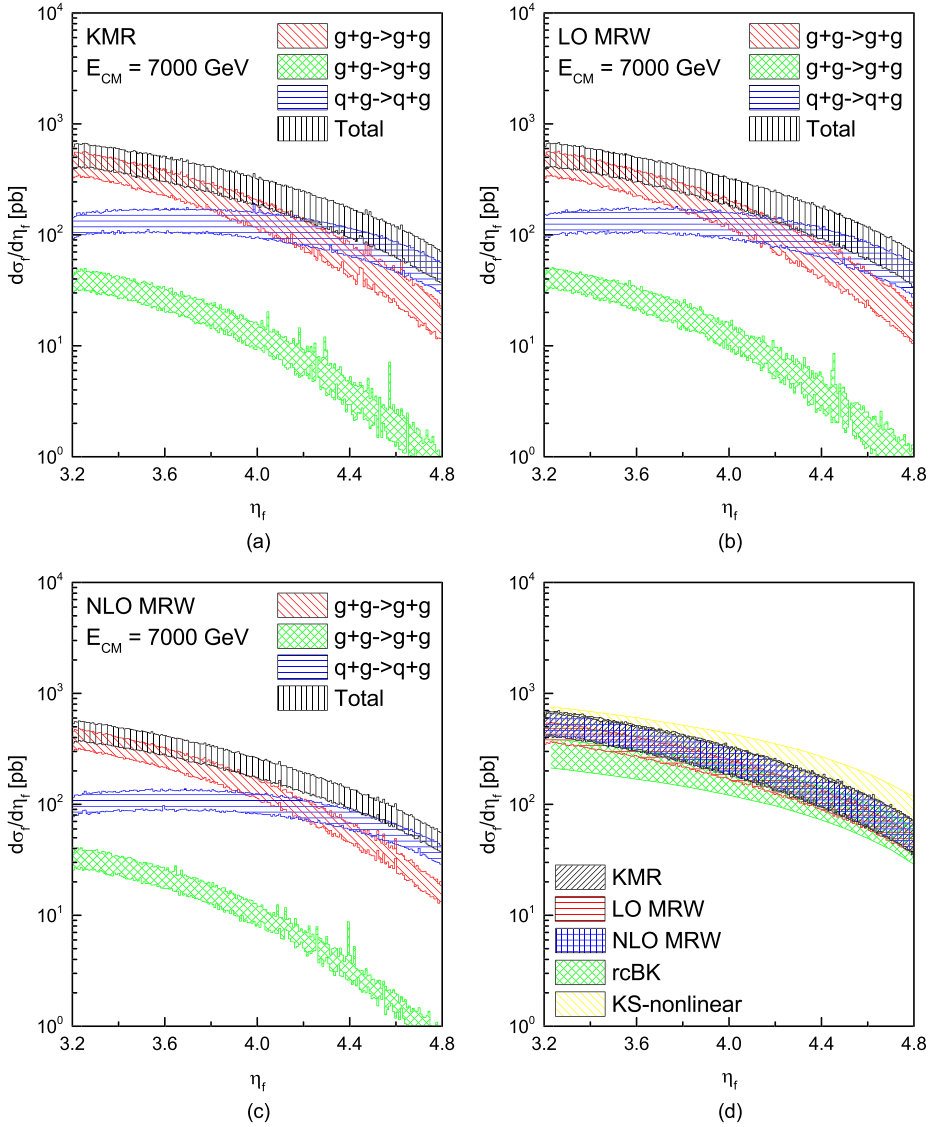


Fig. 11. The calculated predictions regarding the dependency of the differential cross-section for the production of forward-forward di-jets to rapidity of the produced jets, using the *UPDF* of k_t -factorization for $E_{CM} = 7$ TeV. The notion on the diagrams are as in the Fig. 9. In the panel (d), we have compared our results with the predictions made using the *rcBK* and non linear *KS TMD PDF* from the reference [46].

accordance with the *BFKL* iterative evolution equation. In the absence of any experimental data, we refrain ourselves from any assessments regarding these results. Nevertheless, the predictions of the *KMR* scheme (because of its previous success) may provide a base line for a sound comparison. Also, the singular behavior of the *NLO MRW* results may appear undesirable.

Similar predictions are presented in the Figs. 10 and 11, describing the dependency of the differential cross-section of the forward-forward di-jet production, to the angle of the produced

jets ($d\sigma_f/d\Delta\varphi$ to $\Delta\varphi$ in the Fig. 10) and to their rapidity ($d\sigma_f/d\eta_f$ to η_f in the Fig. 11). The notions of these diagrams are as in the Fig. 9. The panel (d) of each figure includes the comparison of the k_t -factorization results to the existing results in the $rcBK$ and the KS frameworks. The irregular behavior of the NLO MRW scheme in both cases, manifests itself in the form of lower values of the predicted differential cross-section. Again, the reliability of these predictions lies within the excellent credit of the KMR $UPDF$ in describing the high energy QCD events.

We should make this note that the use of the hybrid framework, as it was done in present calculation, for the forward-central calculation is safe since the central region x -sector is large enough and the results are compatible with data. However, some recent developments (see the reference [55,56]) have taken into account the quadrupole contribution to the double inclusive jet production. These frameworks have been developed for $p + A$ (proton–heavy ion) scatterings but the saturation scale introduces universality so that at some values of x , the nucleus and nucleon behave similarly. Note that since in the KS -nonlinear equations [44] (the case of dilute projectiles scattering on a dense target), is an effective TMD factorization which utilizes the nonlinear gluon densities to calculate high energy $p + p$ and $p + A$ collisions, the contributions of the final state soft gluon exchanges from both the projectile and the target have been neglected. To find discussions regarding above topic, see [55,56].

In summary, throughout this work, we have tested the $UPDF$ of the k_t -factorization, namely the KMR and MRW formalisms in the LO and the NLO , calculating the production rate of the di-jet pairs at the deep inelastic QCD collisions in the forward-center rapidity sector, compared the results to the existing experimental data of the CMS collaborations and to the results of other frameworks. Through our analysis we have suggested that despite the theoretical advantages of the MRW formalism, the KMR approach performs as good as (if not better) behavior toward describing the experimental data. This is in general agreement with our previous findings, the references [33–41]. Additionally, one can clearly see that the KMR or MRW prescription work better than the KS in describing the experiment. Based on these observations one concludes that the hard-scale dependence should be necessarily included in TMD analysis. Similar observation also have been made previously in the reference [46], showing that introducing Sudakov form factor improves the description of the forward-central jets data. Our results are consistent with this observation. The importance of introducing Sudakov form factor in the production of forward-forward jets have been also discussed in [61]. Furthermore, we have predicted the results of the similar events in the forward-forward rapidity region, relying on the previous success of the $UPDF$ of the k_t -factorization.

Acknowledgements

MM would like to acknowledge the Research Council of University of Tehran and Institute for Research and Planning in Higher Education for the grants provided for him.

MRM sincerely thanks N. Darvishi for valuable discussions and comments. *MRM* extends his gratitude towards his kind hosts at the Institute of Nuclear Physics, Polish Academy of Science for their hospitality during his visit. He also acknowledges the Ministry of Science, Research and Technology of Iran that funded his visit.

Appendix A. The $UPDF$ calculations in the k_t -factorization framework

During a high energy hadronic collision, the involving partons, i.e. the partons that appear at the top of their respective evolution ladders, carry some inherently induced transverse mo-

mentum, as the remnant of the successive (an potentially infinite) number of evolution steps. When working within the framework of collinear factorization, such transverse momentum dependency, due to the assumption of the strong ordering that is embedded in the *LO DGLAP* evolution equation, is conventionally neglected, i.e.,

$$k_{t,i-2}^2 \ll k_{t,i-1}^2 \ll k_{t,i}^2 \ll \dots \ll k_{t,n}^2 \ll \mu^2.$$

Avoiding such assumption, one can include the contributions coming from the transverse momentum distributions of the partons, using either the solutions of the *CCFM* evolution equation or unify the *BFKL* and the *DGLAP* single-scaled evolution equations to form a properly tuned k_t -dependent framework, [57,58]. Utilizing these methods does not always come easy, since these frameworks are mathematically complex and in the case of *CCFM* it is not enough to include all of the contributing sub-processes. Alternatively, the single-scaled *PDF* of the *DGLAP* evolution equation can be convoluted with the required k_t -dependency during the last step of the evolution [15], postulating that:

$$k_{t,i-2}^2 \ll k_{t,i-1}^2 \ll k_{t,i}^2 \ll \dots \ll k_{t,n}^2 \sim \mu^2.$$

Defining a set of reliable and easy to calculate *UPDF* in the k_t factorization framework, the first choice is the so called the *KMR* prescription. Introducing the virtual (loop) contributions via the Sudakov form factor,

$$T_a(k_t^2, \mu^2) = \exp \left(- \int_{k_t^2}^{\mu^2} \frac{\alpha_S(k^2)}{2\pi} \frac{dk^2}{k^2} \sum_{b=q,g} \int_0^{1-\Delta} dz' P_{ab}^{(LO)}(z') \right), \tag{A.1}$$

Kimber et al. [15] have defined the *UPDF* of *KMR* as follows:

$$f_a(x, k_t^2, \mu^2) = T_a(k_t^2, \mu^2) \sum_{b=q,g} \left[\frac{\alpha_S(k_t^2)}{2\pi} \int_x^{1-\Delta} dz P_{ab}^{(LO)}(z) b \left(\frac{x}{z}, k_t^2 \right) \right]. \tag{A.2}$$

$P_{ab}^{(LO)}(z = x/x')$, the *LO* splitting functions [5,12,13], parameterize the probability of evolving from a scale k_t to a higher scale μ without any parton emissions. Naturally, the *NLO* extensions of these functions would take more complicated forms, see the following equation (A.7) in relation to the *MRW* prescriptions. The infra-red cut-off $\Delta = k_t/(\mu + k_t)$ represents a visualization of the *AOC*, which automatically excludes the $x = x'$ point from the range of z -integration blocking the soft gluon singularities that arise from the $1/(1-z)$ terms in the splitting functions.

One immediately notes that throughout the above definition, the k_t -dependency gets introduced into the *UPDF*, only at the last step of the evolution. In order to produce these *UPDF*, the single scaled $b(x, k_t^2)$ functions can be obtained from the *MMHT2014* library [50], where the calculation of the single-scaled functions have been carried out using the *IS* data on the F_2 structure function of the proton. Additionally, using the constraint,

$$T_a(k_t^2 \geq \mu^2, \mu^2) = 1,$$

provides the *KMR* formalism with a smooth behavior over the small- x region, where the $\alpha_S \ln(1/x)$ effects dominate and the *BFKL* evolution equation becomes important. The reader should notice that in the $k_t > \mu$ domain, the unintegrated quark densities of the *KMR* approach are non-vanishing, these parton density functions are considered to be in the *LO* level.

The second option is the *MRW* procedure. The *UPDF* of *KMR*, despite being proven to have physical value, suffers a miss-alignment with the theory of the color coherent radiations, since the *AOC* is a by-product of the successive gluonic emissions, therefore, its manifestation (the infra-red cut-off Δ), should only act on $P_{qq}(z)$ and $P_{gg}(z)$ splitting functions, i.e. the terms including the on-shell gluon emissions. Correcting this problem, *Martin* et al. defined the *MRW* unintegrated densities in the *LO* through the following definitions [13]

$$f_q^{LO}(x, k_t^2, \mu^2) = T_q(k_t^2, \mu^2) \frac{\alpha_S(k_t^2)}{2\pi} \int_x^1 dz \left[P_{qq}^{(LO)}(z) \frac{x}{z} q\left(\frac{x}{z}, k_t^2\right) \Theta\left(\frac{\mu}{\mu + k_t} - z\right) + P_{qg}^{(LO)}(z) \frac{x}{z} g\left(\frac{x}{z}, k_t^2\right) \right], \tag{A.3}$$

and

$$f_g^{LO}(x, k_t^2, \mu^2) = T_g(k_t^2, \mu^2) \frac{\alpha_S(k_t^2)}{2\pi} \int_x^1 dz \left[P_{gq}^{(LO)}(z) \sum_q \frac{x}{z} q\left(\frac{x}{z}, k_t^2\right) + P_{gg}^{(LO)}(z) \frac{x}{z} g\left(\frac{x}{z}, k_t^2\right) \Theta\left(\frac{\mu}{\mu + k_t} - z\right) \right], \tag{A.4}$$

with the modified loop contributions

$$T_q(k_t^2, \mu^2) = \exp\left(-\int_{k_t^2}^{\mu^2} \frac{\alpha_S(k^2)}{2\pi} \frac{dk^2}{k^2} \int_0^{z_{max}} dz' P_{qq}^{(LO)}(z')\right), \tag{A.5}$$

and

$$T_g(k_t^2, \mu^2) = \exp\left(-\int_{k_t^2}^{\mu^2} \frac{\alpha_S(k^2)}{2\pi} \frac{dk^2}{k^2} \left[\int_{z_{min}}^{z_{max}} dz' z' P_{gg}^{(LO)}(z') + n_f \int_0^1 dz' P_{qg}^{(LO)}(z') \right]\right), \tag{A.6}$$

where $z_{max} = 1 - z_{min} = \mu/(\mu + k_t)$ [59]. To a good approximation, include the main kinematics of partonic evolution are included in both of the *UPDF* of *KMR* and *MRW*. Interestingly, the particular choice of the *AOC* in the *KMR* formalism, despite being of the *LO*, includes some higher order contributions, i.e. from the $\ln(1/x)$ -dominant sector. On the other hand, in the *MRW* case, the extension to the higher order levels must be inserted by the means of extra constraints.

To include the *NLO* corrections into the *LO MRW* framework, one needs to define the *NLO* splitting functions as,

$$\tilde{P}_{ab}^{(LO+NLO)}(z) = \tilde{P}_{ab}^{(LO)}(z) + \frac{\alpha_S}{2\pi} \tilde{P}_{ab}^{(NLO)}(z), \tag{A.7}$$

with

$$\tilde{P}_{ab}^{(i)}(z) = P_{ab}^i(z) - \Theta(z - (1 - \Delta')) \delta_{ab} F_{ab}^i P_{ab}(z), \tag{A.8}$$

where $i = 0$ and 1 correspond to the *LO* and the *NLO* levels, respectively. It has been argued that, applying the approximation $P^{(LO+NLO)}(z) \sim P^{(LO)}(z)$ will simplify the *NLO* prescription and

have a negligible effect on the outcome [13], therefore we do not need to express the exact forms of the *NLO* splitting functions. Consequently, the introduction of the *AOC* into the *NLO MRW* formalism is through the extended splitting functions and the $\Theta(z - (1 - \Delta'))$ constraint, with Δ' being defined as:

$$\Delta' = \frac{k\sqrt{1-z}}{k\sqrt{1-z} + \mu}.$$

Additionally, one have to cut off the tail of the probability into the $k_t > \mu$ region by inserting a secondary *AOC* related term into the body of the real emission sector,

$$f_a^{NLO}(x, k_t^2, \mu^2) = \int_x^1 dz T_a \left(k^2 = \frac{k_t^2}{(1-z)}, \mu^2 \right) \frac{\alpha_S(k^2)}{2\pi} \sum_{b=q,g} \tilde{P}_{ab}^{(LO+NLO)}(z) \times b^{NLO} \left(\frac{x}{z}, k^2 \right) \Theta \left(1 - z - \frac{k_t^2}{\mu^2} \right). \quad (\text{A.9})$$

The *Sudakov* form factors in this framework are formulated as:

$$T_q(k^2, \mu^2) = \exp \left(- \int_{k^2}^{\mu^2} \frac{\alpha_S(q^2)}{2\pi} \frac{dq^2}{q^2} \int_0^1 dz' z' \left[\tilde{P}_{qq}^{(0+1)}(z') + \tilde{P}_{gq}^{(0+1)}(z') \right] \right), \quad (\text{A.10})$$

$$T_g(k^2, \mu^2) = \exp \left(- \int_{k^2}^{\mu^2} \frac{\alpha_S(q^2)}{2\pi} \frac{dq^2}{q^2} \int_0^1 dz' z' \left[\tilde{P}_{gg}^{(0+1)}(z') + 2n_f \tilde{P}_{qg}^{(0+1)}(z') \right] \right). \quad (\text{A.11})$$

The reader can find a comprehensive description of the *NLO* splitting functions in the references [13,60].

In the Fig. 1, the gluonic *UPDF* of the k_t -factorization are plotted against the fractional longitudinal momentum of the parent hadron (x) and the transverse momentum of the parton, appearing on the top of the evolution ladder (k_t). The obvious differences in the behavior of the *UPDF* in different frameworks are a direct consequence of employing different manifestations of the *AOC* in their respective definitions.

References

- [1] V.N. Gribov, L.N. Lipatov, *Yad. Fiz.* 15 (1972) 781.
- [2] L.N. Lipatov, *Sov. J. Nucl. Phys.* 20 (1975) 94.
- [3] G. Altarelli, G. Parisi, *Nucl. Phys. B* 126 (1977) 298.
- [4] Y.L. Dokshitzer, *Sov. Phys. JETP* 46 (1977) 641.
- [5] J. Collins, *Foundation of Perturbative QCD*, Cambridge Press, 2011.
- [6] L.V. Gribov, E.M. Levin, M.G. Ryskin, *Phys. Rep.* 100 (1983) 1.
- [7] E.M. Levin, M.G. Ryskin, Yu.M. Shabelsky, A.G. Shuvaev, *Sov. J. Nucl. Phys.* 53 (1991) 657.
- [8] S. Catani, M. Ciafaloni, F. Hautmann, *Phys. Lett. B* 242 (1990) 97.
- [9] S. Catani, M. Ciafaloni, F. Hautmann, *Nucl. Phys. B* 366 (1991) 135.
- [10] J.C. Collins, R.K. Ellis, *Nucl. Phys. B* 360 (1991) 3.
- [11] G. Watt, A.D. Martin, M.G. Ryskin, *Eur. Phys. J. C* 31 (2003) 73.
- [12] M.A. Kimber, A.D. Martin, M.G. Ryskin, *Phys. Rev. D* 63 (2001) 114027.
- [13] A.D. Martin, M.G. Ryskin, G. Watt, *Eur. Phys. J. C* 66 (2010) 163.
- [14] M.A. Kimber, J. Kwiecinski, A.D. Martin, A.M. Stasto, *Phys. Rev. D* 62 (2000) 094006.

- [15] M.A. Kimber, Unintegrated Parton Distributions, Ph.D. thesis, University of Durham, U.K., 2001.
- [16] G. Watt, A.D. Martin, M.G. Ryskin, *Phys. Rev. D* 70 (2004) 014012.
- [17] M. Ciafaloni, *Nucl. Phys. B* 296 (1988) 49.
- [18] S. Catani, F. Fiorani, G. Marchesini, *Phys. Lett. B* 234 (1990) 339.
- [19] S. Catani, F. Fiorani, G. Marchesini, *Nucl. Phys. B* 336 (1990) 18.
- [20] M.G. Marchesini, in: L. Cifarelli, Yu.L. Dokshitzer (Eds.), *Proceedings of the Workshop QCD at 200 TeV*, Erice, Italy, Plenum, New York, 1992, p. 183.
- [21] G. Marchesini, *Nucl. Phys. B* 445 (1995) 49.
- [22] V.S. Fadin, E.A. Kuraev, L.N. Lipatov, *Phys. Lett. B* 60 (1975) 50.
- [23] L.N. Lipatov, *Sov. J. Nucl. Phys.* 23 (1976) 642.
- [24] E.A. Kuraev, L.N. Lipatov, V.S. Fadin, *Sov. Phys. JETP* 44 (1976) 45.
- [25] E.A. Kuraev, L.N. Lipatov, V.S. Fadin, *Sov. Phys. JETP* 45 (1977) 199.
- [26] Ya.Ya. Balitsky, L.N. Lipatov, *Sov. J. Nucl. Phys.* 28 (1978) 822.
- [27] J. Kwiecinski, A.D. Martin, P.J. Sutton, *Phys. Rev. D* 52 (1995) 1445.
- [28] H. Jung, *Comput. Phys. Commun.* 143 (2002) 100–111.
- [29] H. Jung, et al., *Eur. Phys. J. C* 70 (2010) 1237–1249.
- [30] F. Hautmann, M. Hentschinski, H. Jung, arXiv:1207.6420 [hep-ph].
- [31] F. Hautmann, H. Jung, S. Taheri Monfared, *Eur. Phys. J. C* 74 (2014) 3082.
- [32] O. Gituliar, M. Hentschinski, K. Kutak, *J. High Energy Phys.* 1601 (2016) 181.
- [33] M. Modarres, H. Hosseinkhani, *Nucl. Phys. A* 815 (2009) 40.
- [34] M. Modarres, H. Hosseinkhani, *Few-Body Syst.* 47 (2010) 237.
- [35] H. Hosseinkhani, M. Modarres, *Phys. Lett. B* 694 (2011) 355.
- [36] H. Hosseinkhani, M. Modarres, *Phys. Lett. B* 708 (2012) 75.
- [37] M. Modarres, H. Hosseinkhani, N. Olanj, *Nucl. Phys. A* 902 (2013) 21.
- [38] M. Modarres, H. Hosseinkhani, N. Olanj, *Phys. Rev. D* 89 (2014) 034015.
- [39] M. Modarres, H. Hosseinkhani, N. Olanj, M.R. Masouminia, *Eur. Phys. J. C* 75 (2015) 556.
- [40] M. Modarres, M.R. Masouminia, H. Hosseinkhani, N. Olanj, *Nucl. Phys. A* 945 (2016) 168.
- [41] M. Modarres, M.R. Masouminia, R. Aminzadeh Nik, H. Hosseinkhani, N. Olanj, *Phys. Rev. D* 94 (2016) 0744035.
- [42] K. Kutak, J. Kwiecinski, *Eur. Phys. J. C* 29 (2003) 521, arXiv:hep-ph/0303209.
- [43] M. Deak, F. Hautmann, H. Jung, K. Kutak, arXiv:1012.6037 [hep-ph].
- [44] K. Kutak, S. Sapeta, *Phys. Rev. D* 86 (2012) 094043.
- [45] M. Deak, F. Hautmann, H. Jung, K. Kutak, *J. High Energy Phys.* 0909 (2009) 121.
- [46] A. van Hameren, P. Kotko, K. Kutak, S. Sapeta, *Phys. Lett. B* 737 (2014) 335.
- [47] S. Sapeta, *Prog. Part. Nucl. Phys.* 89 (2016) 1.
- [48] CMS Collaboration, CMS-PAS-FSQ-12-008, 2014.
- [49] CMS Collaboration, CMS-PAS-FWD-10-006, 2011.
- [50] L.A. Harland-Lang, A.D. Martin, P. Motylinski, R.S. Thorne, *Eur. Phys. J. C* 75 (2015) 204.
- [51] M. Cacciari, G.P. Salam, G. Soyez, *J. High Energy Phys.* 0804 (2008) 063.
- [52] M. Bury, M. Deak, K. Kutak, S. Sapeta, arXiv:1604.01305 [hep-ph].
- [53] I. Balitsky, *Nucl. Phys. B* 463 (1996) 99.
- [54] Y.V. Kovchegov, *Phys. Rev. D* 60 (1999) 034008.
- [55] F. Dominguez, C. Marquet, B. Xiao, F. Yuan, *Phys. Rev. D* 83 (2011) 105005.
- [56] P. Kotko, K. Kutak, C. Marquet, E. Petreska, S. Sapeta (CERN), A. van Hameren, *J. High Energy Phys.* 1509 (2015) 106.
- [57] J. Kwiecinski, A.D. Martin, A.M. Stasto, *Phys. Rev. D* 56 (1997) 3991.
- [58] K. Golec-Biernat, A.M. Stasto, *Phys. Rev. D* 80 (2009) 014006.
- [59] G. Watt, Parton Distributions, Ph.D. thesis, University of Durham, U.K., 2004.
- [60] W. Furmanski, R. Petronzio, *Phys. Lett. B* 97 (1980) 437.
- [61] K. Kutak, *J. High Energy Phys.* 1212 (2012) 033.